







Colossal dielectric, relaxor ferroelectric, diamagnetic and weak ferromagnetic properties of NdCrO₃ perovskite nanoparticles

Jada Shanker^{1,*} , M. Buchi Suresh² , G. Narsinga Rao³ , and D. Suresh Babu¹ 

¹Department of Physics, Osmania University, Hyderabad, Telangana, India

²International Advanced Research Centre for Powder Metallurgy and New Materials (ARCI), Hyderabad, Telangana, India

³H&S Department, Marri Laxman Reddy Institute of Technology and Management, Hyderabad, Telangana, India

Received: 7 September 2018

Accepted: 2 December 2018

Published online:

19 December 2018

© Springer Science+Business Media, LLC, part of Springer Nature 2018

ABSTRACT

The NdCrO₃ perovskite nanoparticles have been successfully synthesized using sol-gel auto-combustion process. Structural and morphological characterizations of the material have been performed at room temperature using XRD and SEM, respectively. Frequency- and temperature-dependent dielectric measurements have been performed in the range of 1 Hz–10 MHz and RT – 300 °C, respectively. The dielectric constant is found to be in the order of $\epsilon' > 10^3$ at room temperature, indicating the colossal dielectric constant behaviour. Ferroelectric phase transition temperature has increased with an increase in frequency, suggesting that the material is a relaxor ferroelectric nature. Temperature- and field-dependent magnetization measurements have been carried out in the temperature range (5–400 K) and field up to 5 T. M–T curve exhibited a diamagnetic-like behaviour in low temperature and low fields. Two magnetic transitions were found at T_{N1} (223 K) and T_{N2} (33 K) which correspond to para to weak ferromagnetic transition and Nd³⁺ spin ordering, respectively. Hysteresis loop noticed weak ferromagnetism.

Introduction

The common regulatory of electricity and magnetism optimistic over multiferroic materials have shown ferroic order-like ferromagnetism or antiferromagnetism and ferroelectricity at the same time [1]. Such materials may be useful in energy-efficient logic, memory and sensing technology by applying an

electric field to switch magnetic properties and vice versa. Some of perovskite materials may exhibit these properties in which magnetization is induced due to an applied electric field without conducting the flow of current, and therefore, this mechanism might be greatly interesting. For the improvement in multifunctional devices, materials should have strong

Address correspondence to E-mail: jadashanker.phd@gmail.com

coupling between magnetic and electrical orders at room temperature.

In ABO_3 perovskite ceramic compounds, A-site (3^+) cation (rare earth) influences the physical properties over steric effects, and B-site (3^+) cation (transition metal) with its size, valence and spin performs the main role in electric, magnetic and multiferroic properties [2]. The magnetic strength interactions between the A–A-, A–B-, B–B-site cations were frequently found in ABO_3 materials and are increasing in order, respectively, which depends on the electron configuration, the bonding strength, the bond lengths and the bond angles [3]. The strength of the magnetic interactions depends on substitution of rare earth, transition metal cations in their A-, B-site cation positions, respectively. Generally, ortho-chromites show antiferromagnetic behaviour with Neel temperature (T_N) in the range 218–282 K [4]. The magneto-electrical materials have sustained in an improvement in industrial applications. In recent years, $RCrO_3$ ($R = La, Pr, Sm, Nd, Gd, Dy, Er$) materials have shown potential multiferroic properties; the magnetic ordering of 3d spins of transition metal ions and 4f moments of rare earth ions also play a vital role in magneto-electric coupling through lattice distortion. However, these materials have shown promising applications such as ferroelectric, random access memory, multilayer ceramic capacitors and magnetic field sensors [5].

Recently, the authors have studied structural, morphological and electrical properties of $GdCrO_3$, $ErCrO_3$ perovskite materials. All these compounds have indicated the orthorhombic symmetry, and particle size is below 100 nm [6, 7]. The dielectric constant values of $LaCrO_3$, $GdCrO_3$ and $ErCrO_3$ perovskite nanoparticles have been estimated at room temperature, 100 Hz, using impedance spectroscopy and have found to be in the order of 3×10^5 [5], 10^3 [6] and 4×10^3 [7]. The present dielectric constant study of $NdCrO_3$ compound at RT, 100 Hz, has showed in the order of 10^5 . The $RCrO_3$ materials have exhibited high electrical conductivity, high densification, high temperature durability in reducing atmosphere and good physical and chemical stability which are the required properties for SOFC applications [8, 9]. From this study, the authors have concluded that $NdCrO_3$ material is also a potential candidate for colossal dielectric capacitor and SOFC applications.

Researchers have used various synthesis techniques to prepare ABO_3 -type perovskite materials. These include solid-state reaction, co-precipitation, solution-gel, precursor, hydrothermal, sol-gel, citrate-gel, sol-gel auto-combustion methods; among these techniques, the authors have adapted sol-gel auto-combustion technique to prepare $NdCrO_3$ perovskite compound, due to numerous advantages; for example, it makes homogeneity of a compound and reduced the impurity; therefore, single-phase formation has been confirmed. In addition, controlling the particle size in nanoscale, resulting nano particles were produced [6, 7]. Nanoparticles of compound have more effect on their structural, electrical and magnetic properties, and they have shown enhanced properties than the micro-, milliseize particles of compound. The nanoparticles of grain boundaries are closer (i.e. very less gaps are found between grain boundaries) than the micro-, milliseize particles of the compound. While taking the measurements in the presence of different fields (electrical/magnetic), temperatures and frequencies, the nanoparticles of material can give exact physical and chemical properties than the other size of the particles of material. Moreover, if we repeat the measurements on same nanoparticle compound, we can achieve the same previous results, but in the case of micro-, milliseize particles of compound we may not achieve the same results.

In this paper, the authors have explained detailed structural, electrical and magnetic properties of the $NdCrO_3$ nanoparticles to understand the magnetic and electric properties.

Experimental procedure

Polycrystalline powder of $NdCrO_3$ perovskite compound has been prepared using sol-gel auto-combustion technique. The required chemicals for synthesis are presented in Table 1. For making $NdCrO_3$, we have taken 1:1:3 molar ratio of stoichiometric amounts of Nd_2O_3 , $Cr(NO_3)_3 \cdot 9H_2O$ and citric acid which were taken separately. Nd_2O_3 was converted to neodymium nitrate using HNO_3 . Double distilled water has been used to dissolve the stoichiometric amount of raw materials individually and mixed using magnetic stirrer for homogeneous solution, and then, NH_3 was added to keep the PH value of mixed solution at 7. This mixed solution was

Table 1 Chemicals used to synthesize NdCrO₃ perovskite by sol–gel auto-combustion method

Chemical name	Molecular weight	Purity (%)	Grade	Make
Nd ₂ O ₃	336.477	99.99	–	Indian rare earth
HNO ₃	63.01	69	AR	SD Fine
Cr(NO ₃) ₃ ·9H ₂ O	400.15	98	GR	LOBA
C ₆ H ₈ O ₇ ·H ₂ O	210.14	99.5	GR	MARK
NH ₃	17.03	25	AR	SD Fine
C ₂ H ₆ O ₂	62.07	99	AR	SD Fine

stirred and simultaneously heated (at 150 °C) until the initial amount of solution becomes 1/3; then, ethylene glycol has been added as a fuel to the 1/3 of the initial solution. After few minutes, magnetic bead was removed from the dried gel and the string was stopped, but the heating temperature slowly increased until the resulting gel combusted. The combusted powder was collected and calcined at 750 °C for 4 h. Calcined powder was ground for 4 h to get homogenous nanoparticles. The obtained powder was pelletized under uniaxial pressing. Sintering process is essential in polycrystalline ceramic material, that effect on grain growth and densification [10]. Hence, these pellets have sintered at 900 °C temperature for 4 h. Finally, these sintered pellets have been used for measurements.

SHIMADZU XRD-7000 X-ray diffractometer (XRD) has been used to characterize the phase and the crystallographic structure of the NdCrO₃ perovskite. Microstructure and the grain size distribution of NdCrO₃ sintered pellet have been studied using a scanning electron microscopy (SEM) ZISS EVO-18. Experimental density of NdCrO₃ has been calculated using the Archimedes principle, and also the mass and the volume of the pellets were measured and compared with theoretical density. The SOLARTRON SI1260 model impedance analyser has been used to carry out dielectric and impedance spectroscopic measurements. The silver-coated surfaces were used as electrodes for the dielectric measurements. The MPMS SQUID magnetometer has been used to carry out magnetic measurements. For the magnetic measurements, the dimension of the pellet should be a rectangle shape to avoid correction.

Results and discussion

Structural and morphological analysis

Rietveld refinement software has been used to refine the XRD pattern of the sintered pellet of NdCrO₃ for 15 cycles which is shown in Fig. 1. The evaluated lattice parameters and refinement parameters are given in Table 2. The average crystalline size has been calculated using Debye Scherer formula and was found to be 32 nm.

$$D = \frac{0.94 * \lambda}{\beta \cos \theta}$$

where D is the average crystalline size; λ , X-ray wave length (1.54 Å); β , full width at half maxima; θ , Bragg angle.

Figure 2a shows the SEM microstructure of NdCrO₃ sintered pellet. It has seen that the grain size, grain distribution and certain amount of voids have uniform throughout the surface. The average grain size was found to be order of 80 nm. The density of

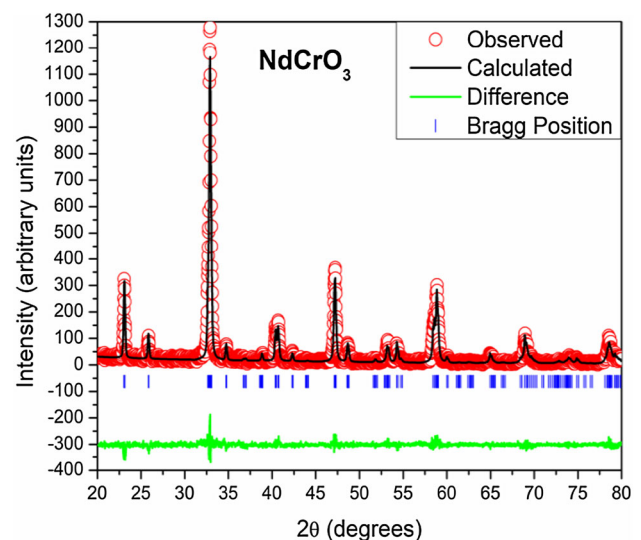
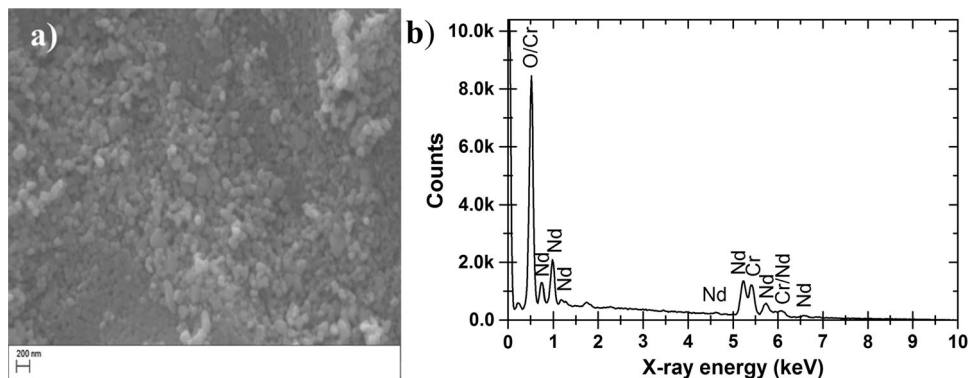


Figure 1 XRD Rietveld refinement of sintered pellet of NdCrO₃ perovskite compound.

Table 2 Lattice parameters and Rietveld refinement parameters of NdCrO₃ sintered pellet

Perovskite	Structure	Lattice parameters (Å°)			$V = a*b*c$	Rietveld refinement parameters				
		a	b	c		R_P	R_{WP}	R_{EXP}	χ^2	GOF
NdCrO ₃	Orthorhombic (Pbnm)	5.422	5.479	7.693	228.585	7.9	9.7	8.4	1.4	1.2

Figure 2 a Scanning electron microscopy (SEM) microstructure and **b** EDEX spectrum of sintered pellet of NdCrO₃ (inset **b** shows EDEX spectrum exported from INCA software as as.emsa file).



the pellet has been calculated and was found to be around 94%. Figure 2b shows the EDEX spectrum of NdCrO₃ sintered pellet and Nd, Cr, O elements, suggesting that the NdCrO₃ synthesized compound has no impurity elements.

Dielectric analysis

The real part of the dielectric constant (ϵ') and dielectric loss ($\tan \delta$) have been calculated from the impedance data using the following relation [11]

$$\epsilon' = \frac{Z''t}{2\pi f A \epsilon_0 (Z'^2 + Z''^2)}$$

$$\tan \delta = \frac{Z'}{Z''}$$

where “ t ” is the thickness of the pellet, “ A ” is the surface area of the pellet, $\epsilon_0 = 8.85 \times 10^{12}$ F/m, real part of impedance (Z'), imaginary part of impedance (Z'').

Frequency variation dielectric constant (ϵ') of NdCrO₃ at various temperatures is shown in Fig. 3. It has been found that dielectric constant (ϵ') decreases with rising frequency for all given temperatures. The dielectric constant (ϵ') was found to be high value in the low frequency region and is decreasing with a rising frequency which is due to the space charge polarization, which leads to the high dielectric constant and expressive frequency dispersion in the low

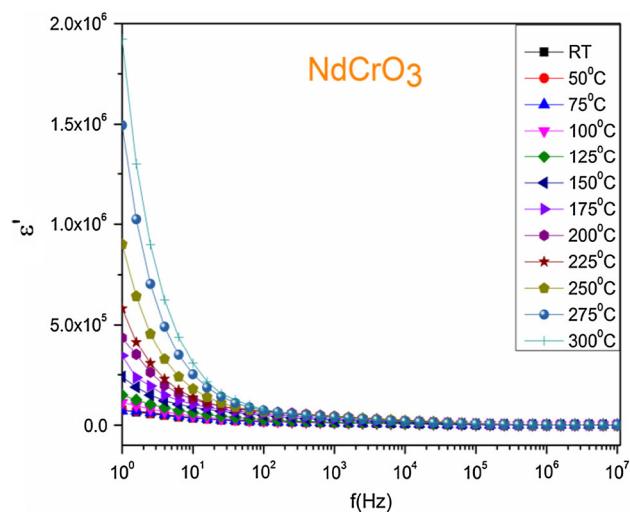


Figure 3 Frequency dependence of the dielectric constant (ϵ') of NdCrO₃ at different temperatures.

frequency region [12–14]. The dielectric constant (ϵ') was found to be increased with increasing temperature. This suggests that the thermally activated nature of the dielectric relaxation exists in this material [14]. It is also observed that the dielectric constant is in the order of $\epsilon' > 10^3$ indicating the colossal behaviour. Generally, ferroelectric and relaxor ferroelectric materials show high dielectric constant ($\epsilon' > 10^3$) [6].

Frequency-dependent dielectric loss ($\tan \delta$) of NdCrO₃ perovskite ceramic compound at different

temperatures is shown in Fig. 4. It shows that dielectric loss ($\tan \delta$) decreases with rising frequency at a given temperature. The dielectric loss ($\tan \delta$) increases with increasing temperature below the 175 °C in the low frequency region and is due strong space charge polarization, more electron exchange between Cr^{3+} - Cr^{3+} through the grain boundary in the direction of applied electric field which leads to partial polarization, and therefore, dielectric loss increased [15]. Beyond 175 °C, dielectric loss ($\tan \delta$) decreases with increasing temperature which may be due to weak space charge polarization in the material [16]. The high value of dielectric loss ($\tan \delta$) observed in the low frequency region corresponds to a low conductivity of the grain boundary. In the high frequency region, loss is constant, which indicates a high conductivity of grain [17].

Figure 5 shows temperature-dependent dielectric constant of NdCrO_3 at various frequencies. It is seen that the dielectric constant is increased with increasing the temperature up to 178 °C at 100 Hz due to increase in drift mobility of charge carriers with an increase in temperature [18], which corresponds to the polar bonds created by displacement of Cr^{3+} (space charge polarization) causing the increase in dielectric constant [19]. Further increasing the temperature dielectric constant decreased, suggesting dielectric anomaly, i.e. a ferroelectric phase transition at 178 °C at 100 Hz. It is clearly seen that the transition temperature increased with increasing frequency

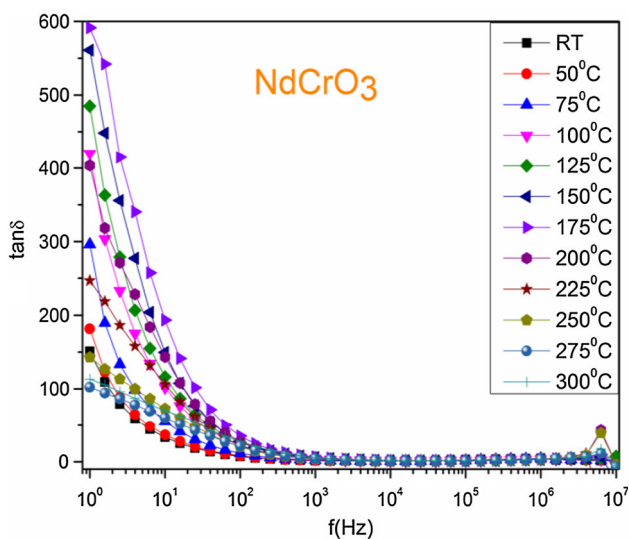


Figure 4 Frequency dependence of the dielectric loss ($\tan \delta$) of NdCrO_3 at different temperatures.

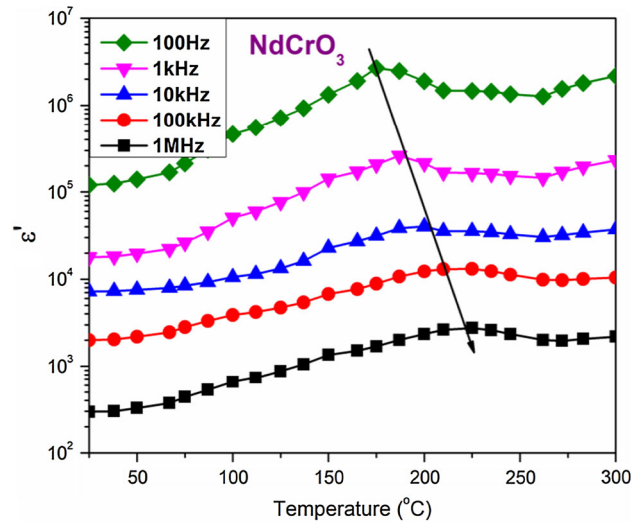


Figure 5 Temperature-dependent dielectric constant of NdCrO_3 at various frequencies.

(225 °C at 1 MHz), suggesting that the material is relaxor ferroelectric [1, 20, 21]. The peak becomes broader with increasing frequency which suggests the presence of diffuse phase transition (DPT) [21, 22].

AC and DC conductivity analysis

The AC conductivity (σ_{ac}) of NdCrO_3 perovskite compound has been evaluated by using the formula [23].

$$\sigma_{ac} = 2\pi f \epsilon_0 \epsilon' \tan \delta$$

where f is the applied frequency (Hz); $\tan \delta$, dielectric loss; ϵ_0 , dielectric constant in free space (8.854×10^{-12} F/m); ϵ' , dielectric constant of the sample.

Figure 6 shows frequency dependence AC conductivity plots of NdCrO_3 perovskite at various temperatures. The AC conductivity (σ_{ac}) remained constant (plateau region) at lower frequencies and increased rapidly with increasing temperature at higher frequencies; the low and high frequency region plots follow the universal power law $\sigma_{ac} \propto f^n$ relation [24], where “n” represents the exponential factor. This kind of behaviour is often seen in mixed oxide material perovskite ceramic material [6, 24, 25]. The AC conductivity curves of the NdCrO_3 perovskite ceramic material follow the Jonscher’s power law [25].

$$\sigma_{ac} = \sigma_{dc} + A\omega^n$$

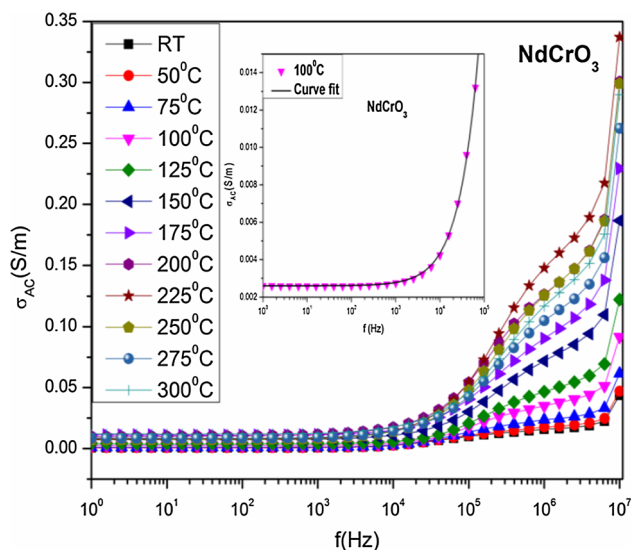


Figure 6 Frequency dependence AC conductivity (σ_{ac}) Plots of NdCrO_3 at different temperatures.

where n is the frequency exponent in the range of $0 \leq n \leq 1$.

The plateau region of the plot corresponds to the frequency-independent part related to DC conductivity (σ_{dc}), and a dispersive region corresponds to the frequency-dependent part ($A\omega^n$) which is related to AC conductivity. The hopping frequency (ω) is obtained at the point where the slope changes in the conductivity spectrum. The Jonscher's power law parameters are evaluated by nonlinear curve fitting as shown in Fig. 6 and presented in Table 3. The conductivity increases with an increase in

Table 3 Jonscher's power law parameters of NdCrO_3 sintered pellet

Temperature (°C)	σ_{dc} (S/m)	A	ω	n
RT	0.0006	4E-7	25924	0.92
50	0.0007	3E-7	39935	0.95
75	0.0011	3E-7	64679	0.96
100	0.0026	2E-7	66231	0.98
125	0.0040	3E-7	64716	0.95
150	0.0074	1E-6	16009	0.88
175	0.0110	2E-7	10191	1.00
200	0.0102	2E-6	4040	0.87
225	0.0080	1E-6	6283	0.96
250	0.0073	2E-6	6408	0.91
275	0.0085	1E-6	6283	0.95
300	0.0121	8E-7	4084	0.97

temperature which reveals the thermally activated electrical conduction in the material [14, 26–29].

Magnetic analysis

Figure 7a, b shows the temperature-dependent magnetization curve (ZFC and FC) of NdCrO_3 at 0.01 T and 0.5 T applied field, respectively. In Fig. 7a, MT curves have shown interesting complex behaviour. The FC and ZFC curves are nearly symmetric with an opposite sign at low temperature. The FC magnetization curve is in the positive region from 5 to 400 K and decreases with increasing temperature. The ZFC magnetization curve has shown negative values at low temperatures, and the magnitude decreased with an increase in temperature. ZFC magnetization sign changes from positive at high temperature (> 223 K) to negative at low temperature (< 223 K) region which indicates the transition from paramagnetic to diamagnetic behaviour. A novel “diamagnetism-like” behaviour has been observed in the low temperature region for the first time in NdCrO_3 perovskite. As applied magnetic field increases, the negative magnetization disappears and it becomes positive at 0.5 T as shown in Fig. 7b and this kind of behaviour is observed in PrCrO_3 , HoCrO_3 [30–32]. This kind of behaviour originates from an antiparallel orientation of the weak ferromagnetic moments of Cr^{3+} and of Nd^{3+} ions. It has been seen that there exist two magnetic transitions T_{N1} and T_{N2} at 223 K and 33 K, respectively. The first transition temperature T_{N1} (223 K) corresponds to para magnetism at high temperature to weak ferromagnetism at low temperature. The orthorhombic structure of RCrO_3 systems at room temperature has exhibited canted antiferromagnetic with Cr^{3+} magnetic moments with the first transition Neel temperature (T_{N1}) of 112–282 K [1, 32] and dielectric transition (T_c) in the 472–516 K [1]. The second transition seen at T_{N2} (33 K) is due to antiferromagnetic ordering of spin of the rare earth ion. The octahedron structure of CrO_6 favours the super exchange interaction between the large spins of Cr^{3+} ions sandwiched between O^{2-} ions at lower temperatures resulting in antiparallel spins. Due to the variation in the orthorhombic structure of NdCrO_3 , the bond angle between Cr-O-Cr deviates slightly from 180° , which results in residual electron spin originating from the imperfect super exchange interaction and showing canted antiferromagnetic below T_{N1} (223 K). The antiferromagnetic exchange

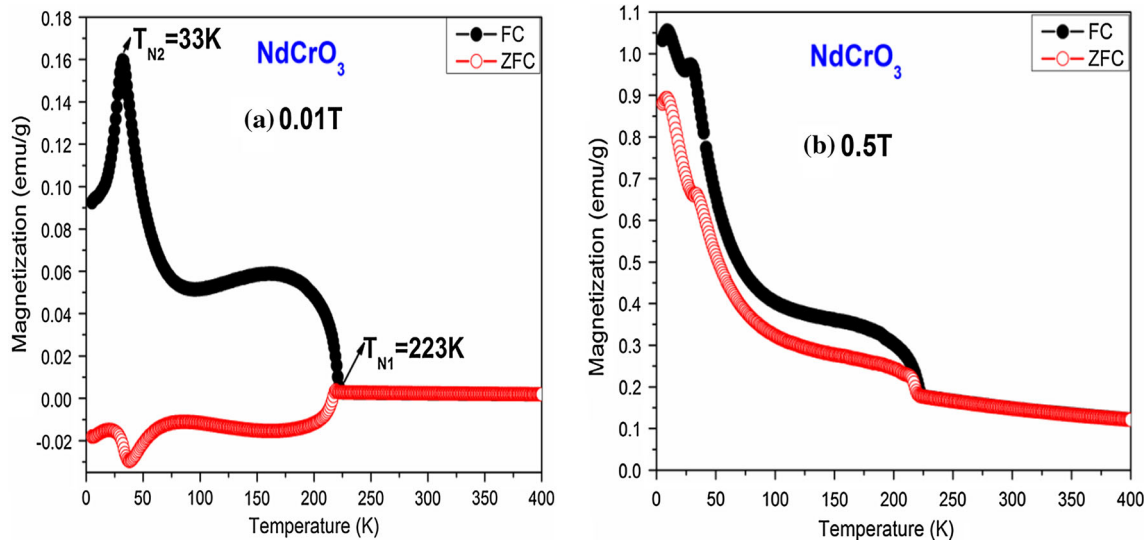


Figure 7 Temperature-dependent magnetization of NdCrO_3 at **a** 0.01 T and **b** 0.5 T magnetic fields.

interaction between Cr^{3+} spins results in a weak ferromagnetic configuration. The Cr and Nd substructures, which are uncoupled, experience the equal magnitude of the external magnetic field in the ZFC mode of magnetization. The total magnetization is the result of independent contribution of Nd and Cr substructures. The Cr^{3+} moments appearing at T_{N1} impose a local field over the Nd^{3+} moments during the FC magnetization mode. The internal field contribution of Cr substructure and the external magnetic field due to the cooling in the presence of the field imposes the field on Nd substructure. Hence, the magnetization contributions of Nd and Cr substructures decrease with increase in temperatures in the FC mode. The second Neel temperature T_{N2} of 33 K results due to Nd^{3+} spin reordering in the antiferromagnetic arrangement [1, 32]. The novel magnetization, i.e. diamagnetism-like behaviour, is seen due to the contribution of two different magnetic groups (Cr and the Nd substructures) with antiferromagnetic and ferromagnetic interactions resulting from the coexistence and competition mechanisms. The magneto-crystalline anisotropy energy and external magnetic field strength competition affect the contribution to magnetization, which results due to spins [32]. At lower values of the measuring fields, the majority of the spins will not be oriented in the direction of the applied magnetic field strength. This difference causes from the antiparallel orientation of the Cr^{3+} weak ferromagnetic moment and of the Nd^{3+} moment by Nd^{3+} – Cr^{3+} exchange

interaction between FC and ZFC magnetization modes. As the external applied magnetic field is increasing, more spins aligned along the direction of the external magnetic field, and hence, the negative magnetization disappears as shown in Fig. 7b.

M–H measurements of the NdCrO_3 perovskite compound have been carried out at 5 K and 300 K shown in Fig. 8a, b, respectively. The hysteresis of NdCrO_3 compound seems to be asymmetric, which corresponds to exchange bias field [32]. The broadening of hysteresis loop seems to be small and has very weak coercive field (H_c) and remanent magnetization (M_r) values. However, it has not shown saturation up to 0.5 T at 5 K and 300 K. The M–H loop of NdCrO_3 nanoparticles shows the weak ferromagnetic nature at room temperature (300 K), and magnetization increases with decreasing the temperature from 300 K to 5 K. The weak ferromagnetic nature of the material increased with decreasing the temperature, due to the generation of residual moment by a canted spin structure of material [18]. The coercive field (H_c) and remanent magnetization (M_r) have been estimated and were found to be 0.112 T, 0.176 emu/g at 5 K and 0.003 T, 0.001 emu/g at 300 K, suggesting the weak ferromagnetic behaviour in the material [21, 33].

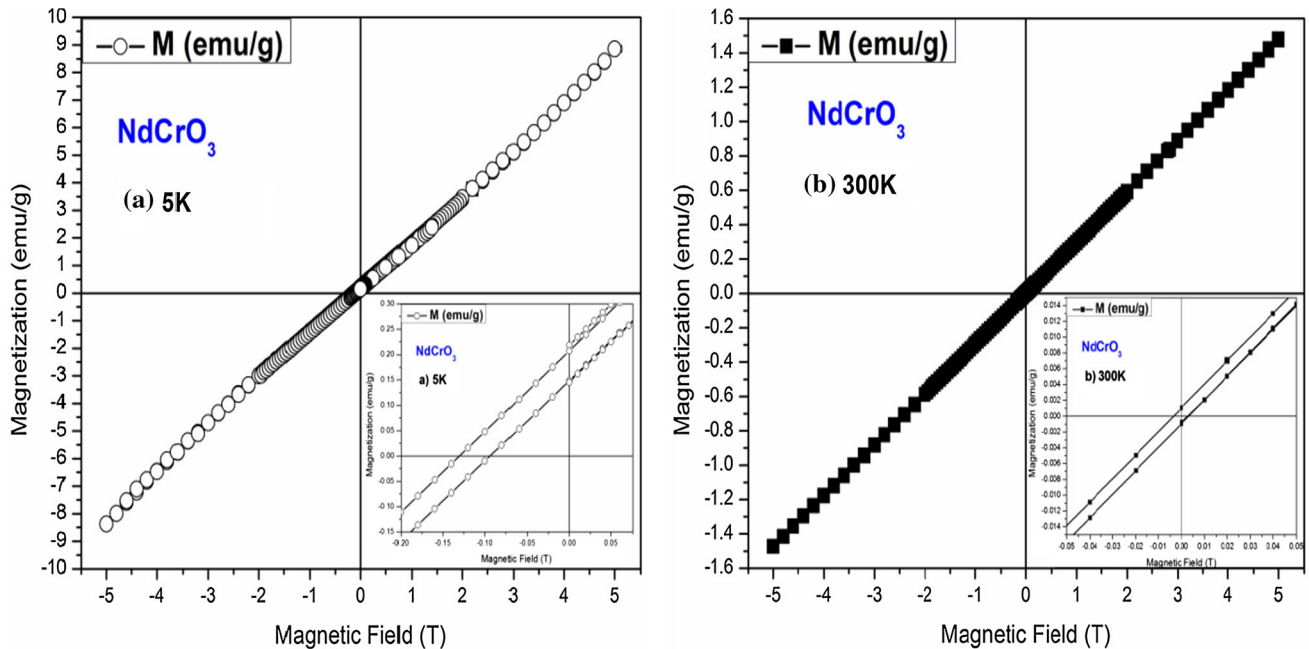


Figure 8 M–H hysteresis loop of NdCrO₃ perovskite at **a** 5 K and **b** 300 K temperatures.

Conclusions

Sol–gel auto-combustion technique has been adapted to synthesize the NdCrO₃ perovskite nanoparticles. The XRD pattern suggested that the sample is single-phase orthorhombic structure, which belongs to Pbnm symmetry. The average crystallite size was calculated and found to be 32 nm. Grains have uniformly distributed over the surface, and average grain size was estimated to be 80 nm. The frequency-dependent conductivity curve followed the Jonsher’s power law. The frequency- and temperature-dependent dielectric constant exhibited colossal dielectric constant value which is in the order of $\epsilon' > 10^3$, and is a mandatory condition for giant capacitors. The frequency-dependent dielectric constant has shown that the material is relaxor ferroelectric in nature and the ferroelectric transition temperature increased with the rise in frequency (i.e. 178 °C at 100 Hz and 225 °C at 1 MHz). M–T curves showed novel “diamagnetic-like behaviour in low temperature and low field region for the first time in NdCrO₃. M–T curves exhibited two transitions at 223 K and 33 K. The transition T_{N1} is related to para to weak ferromagnetic, and the T_{N2} is due to Nd³⁺ spin ordering. M–H curve suggests that the material is a weak ferromagnetic.

Acknowledgements

One of the authors, Jada Shanker, would like to thank SRF-UGC-RGNF for providing financial assistance to carry out this work.

Funding

Funding was provided by University Grants Commission (Grant No. F117.1/201617/RGNF201517SCTEL27682/(SAIII/Website)).

References

- [1] Sahu JR, Serrao CR, Ray N, Waghmar UV, Rao CNR (2007) Rare earth chromites: a new family of multiferroics. *J Mater Chem* 17:42–44
- [2] Ahmad I, Akhtar MJ, Younas M, Siddique M, Hasan MM (2012) Small polaronic hole hopping mechanism and Maxwell-Wagner relaxation in NdFeO₃. *J Appl Phys* 112:074105
- [3] Du Y, Cheng Z, Wang X, Dou SX (2010) Structure, magnetic, and thermal properties of Nd_{1-x}La_xCrO₃ ($0 \leq x \leq 1.0$). *J Appl Phys* 108:093914
- [4] Bora T, Ravi S (2015) Sign reversal of magnetization and tunable exchange bias field in NdCr_{1-x}Fe_xO₃ ($x = 0.05–0.2$). *J Magn Magn Mater* 386:85–91
- [5] Coskun M, Polat O, Coskun FM, Durmus Z, Çağlar M, Turut A (2018) The electrical modulus and other dielectric

- properties by the impedance spectroscopy of LaCrO₃ and LaCr_{0.90}Ir_{0.10}O₃ perovskites. RSC Adv 8:4634–4648
- [6] Shanker J, Venkataramana K, Vittal Prasad B, Vijaya Kumar R, Suresh Babu D (2018) Influence of Fe substitution on structural and electrical properties of Gd orthochromite ceramics. J Alloys Compd 732:314–327
- [7] Shanker J, Buchi Suresh M, Saravanan P, Suresh Babu D (2018) Effects of Fe substitution on structural, electrical and magnetic properties of erbium ortho-chromite nano polycrystalline material. J Magn Magn Mater. <https://doi.org/10.1016/j.jmmm.2018.10.094>
- [8] Shanker J, Buchi Suresh M, Suresh Babu D (2016) Synthesis, characterization and electrical properties of NdXO₃ (X = Cr, Fe) nanoparticles. Mater Today Proc 3:2091–2100
- [9] Polat O, Durmus Z, Coskun FM, Coskun M, Turut A (2018) Engineering the band gap of LaCrO₃ doping with transition metals (Co, Pd, and Ir). J Mater Sci 53:3544–3556. <https://doi.org/10.1007/s10853-017-1773-3>
- [10] Yan LC, Hassan J, Hashim M, Yin WS, Khaoon TF, Jeng WY (2011) Effect of sintering temperatures on the microstructure and dielectric properties of SrTiO₃. World Appl Sci J 14(7):1091–1094
- [11] Khasa S, Singh P, Sanghi S, Singh N, Agarwa A (2014) Structural analysis and dielectric characterization of Aurivillius type CaSrBi₂Nb₂O₉ ceramics. J Integr Sci Technol 2(1):13–21
- [12] Singh NK, Kumar P, Kumar H, Rai R (2010) Structural and dielectric properties of Dy₂(Ba_{0.5}R_{0.5})₂O₇ (R = W, Mo) ceramics. Adv Mater Lett 1(1):79–82
- [13] Sreehari Sastry S, Tanuj Kumar L, Tiong HS (2014) Dielectric studies on benzothiazole based liquid crystals at radio frequency region. Int J Innov Res Sci Eng Technol 3(3):10212–10219
- [14] Barik SK, Choudhary RNP, Singh AK (2011) AC impedance spectroscopy and conductivity studies of Ba_{0.8}Sr_{0.2}TiO₃ ceramics. Adv Mater Lett 2(6):419–424
- [15] Mir SA, Ikram M, Sultan K, Habib Z, Kausar H, Asokan K (2015) Correlative exploration of structural, optical and electric properties of colossal dielectric Ni doped sm orthoferrites. Adv Mater Lett 6(12):1081–1087
- [16] Shrivastav BD, Barde R, Mishra A, Phadake S (2013) Frequency and temperature dependence of dielectric properties of fish scales tissues. Res J Phys Sci 1(6):24–29
- [17] Sing N, Agarwal A, Sanghi S (2011) Dielectric relaxation, conductivity behavior and magnetic properties of Mg Substituted Zn–Li ferrites. Curr Appl Phys 11:783–789
- [18] Jaya Prakash B, Rudramadevi BH, Buddhud S (2014) Analysis of ferroelectric, dielectric and magnetic properties of GdFeO₃ nanoparticle. Ferroelectr Lett Sect 41:110–122
- [19] Kleemann W, Shvartsman VV, Bedanta S, Borisov P, Tkach A, Vilarinho PM (2008) (Sr,Mn)TiO₃-a magnetoelectrically coupled multiglass. J Phys: Condens Matter 20:434216
- [20] Prasad BV, Narsinga Rao G, Chen JW, Suresh Babu D (2011) Relaxor ferroelectric like giant permittivity in PrCrO₃ semiconductor ceramics. Mater Chem Phys 126:918–921
- [21] Miah MJ, Khan MNI, Akther Hossain AKM (2016) Weak ferromagnetism and magnetoelectric effect in multiferroic xBa_{0.95}Sr_{0.05}TiO₃-(1-x)BiFe_{0.9}Gd_{0.1}O₃ relaxors. J Magn Magn Mater 401:600–611
- [22] Dura A, Arevalo-Lopez AM, Castillo-Martinez E, Garcia-Guaderrama M, Moran E, Cruz MP, Fernandez F, Alario-Franco MA (2010) Magneto-thermal and dielectric properties of biferroic YCrO₃ prepared by combustion synthesis. J Solid State Chem 183:1863–1871
- [23] Dashan S, Choudhary RNP, Kumar A (2014) Impedance spectroscopy and conduction mechanism of multiferroic (Bi_{0.6}K_{0.4})(Fe_{0.6}Nb_{0.4})O₃. J Phys Chem Solids 75:1376–1382
- [24] Prasad NV, Chandra Sekhar M, Kumar GS (2008) Impedance spectroscopic studies on lead based perovskite materials. Ferroelectrics 366(1):55–66
- [25] Basu S, Ramesh Babu K, Choudhary RNP (2012) Studies on the piezoelectric and magnetostrictive phase distribution in lead zirconate titanate–cobalt iron oxide composites. Mater Chem Phys 132:570–580
- [26] Shanker J, Buchi Suresh M, Suresh Babu D (2015) Synthesis, characterization and impedance spectroscopy studies of NdFeO₃ perovskite ceramics. Int J Sci Eng Res 3(7):194–197
- [27] Shanker J, Narsinga Rao G, Venkataramana K, Suresh Babu D (2018) Investigation of structural and electrical properties of NdFeO₃ perovskite nanocrystalline. Phys Lett A 382:2974–2977
- [28] Shanker J, Narsinga Rao G, Suresh Babu D (2018) Impedance spectroscopy and permittivity investigation of NdCrO₃ perovskite ceramic nanoparticles. IOP Conf Ser Mater Sci Eng 360:012004
- [29] Shanker J, Vittal Prasad B, Buchi Suresh M, Vijaya Kumar R, Suresh Babu D (2017) Electrical properties of NdCr_{1-x}FexO₃ perovskite ceramic nanoparticles—an impedance spectroscopy studies. Mater Res Bull 94:385–398

- [30] Su Y, Zhang J, Feng Z, Li Z, Shen Y, Cao S (2011) Magnetic properties of rare earth HoCrO_3 chromites. *J Rare Earths* 29(11):1060–1065
- [31] Venugopal Rao B, Vittal Prasad B, Narsinga Rao G, Chou FC, Suresh Babu D (2015) Magnetization reversal in PrCrO_3 . *Adv Mater Res* 1086:96–100
- [32] Wang S, Huang K, Hou C, Yuan L, Xiaofeng W, Dayong L (2015) Low temperature hydrothermal synthesis, structure and magnetic properties of RECrO_3 (RE = La, Pr, Nd, Sm). *Dalton Trans* 44:17201–17208
- [33] Kumar P, Kar M (2014) Effect of structural transition on magnetic and dielectric properties of La and Mn co-substituted BiFeO_3 ceramics. *Mater Chem Phys* 148:968–977